Available online at www.sciencedirect.com

ScienceDirect

journal homepage: www.elsevier.com/locate/he

Investigation of ZrFe$_2$-type materials for metal hydride hydrogen compressor systems by substituting Fe with Cr or V

E.D. Koultoukis [a,b,c,d,*], S.S. Makridis [b,d], E. Pavlidou [c], P. de Rango [e], A.K. Stubos [b]

[a] McPhy Energy S.A., Z.A. Quartier Riétière, La Motte-Fanjas 26190, France
[b] NCSR "Demokritos", Ag. Paraskevi, Athens 15-310, Greece
[c] Department of Physics, Aristotle University of Thessaloniki, Egnatia Street, Thessaloniki, GR 54124, Greece
[d] Institute for Renewable Energy and Environmental Technologies, University of Bolton, Deane Road, Bolton UBL3 5AB, United Kingdom
[e] Institut Néel and CRETA, CNRS, BP 166, 38042 Grenoble Cedex, France

ARTICLE INFO

ABSTRACT

In this study, the effects of partial substitution of Fe, in the ZrFe$_2$-system alloys, by Cr or V are presented. The two studied alloys, ZrFe$_{1.8}$V$_{0.2}$ and ZrFe$_{1.8}$Cr$_{0.2}$, have been synthesized by high frequency induction-levitation melting under inert Ar atmosphere. The induction furnace was equipped with a water-cooled copper crucible that permits the rapid solidification of the alloy after the melting. The crystal structures of the investigated alloys have been studied by the Rietveld analysis of the obtained X-ray diffraction (XRD) patterns. The microstructure has been observed by a scanning electron microscope (SEM) on polished samples of the alloys. Their hydriding properties have been studied with a high pressure Sievert's type apparatus, up to 200 bar. All pressure–composition–temperature (PCT) measurements have been obtained at 20, 60 and 90 °C. Two high temperature activation cycles have been conducted prior to PCT measurements. The results showed almost the same uptake for the alloys after identical activation and lowering of the plateau pressure in both cases.

Introduction

As the public interest on renewable energy solutions increases and as the worldwide oil reserves tend to be less, the solution of hydrogen as energy carrier and fuel (with an on-site production) is becoming more attractive [1]. The main drawback which the scientific community has to overcome is the safe, fast and efficient storage of hydrogen for both onboard and stationary applications [2,3]. Metal hydrides offer the ability to store hydrogen in a very large range of temperatures and pressures. Hydrogen reacts at elevated temperatures with

many transition metals and their alloys to form hydrides. The electropositive elements are the most reactive, i.e. Sc, Yt, lanthanides, actinides, and members from the Ti and V groups. The binary hydrides of the transition metals are predominantly metallic in character and are usually referred to as metallic or graphite-like appearance, and can often be wetted by Hg [4]. One kind of promising hydrogen storage materials are Laves phase compounds having the formula unit AB_2, which demonstrate reasonably high capacities and good cycling stability [5—11]. This class of Laves phase includes the cubic C15 ($MgCu_2$), the hexagonal C14 ($MgZn_2$) and the di-hexagonal C36 ($MgNi_2$) structures. Both C14 and C15 Laves phase structures can store hydrogen in good amounts and thus are much more studied than C36 type alloys [12]. The potential AB_2 types are obtained with Ti and Zr on the A site. The B elements are represented mainly by different combinations of 3d atoms, V, Cr, Mn and Fe [13]. The hydrogen-storage capacity can reach up to 2 wt.% in Laves phase V—7.4%Zr—7.4%Ti—7.4%Ni [14]. The electrochemical studies of Zr-substituted AB_2 alloys reveal that the electrochemical storage capacity increases with increasing the amount of Zr [15]. The presence of excess elements in non-stoichiometric AB_2 alloys leads to the improvement of the storage properties thanks to the introduction of disorder in an unchanged C14 hexagonal structure presenting modified cell parameters [16,17]. $ZrFe_2$ hydrides crystallize in both C14 and C15 Laves phase structures and they present appealing properties so that they could be used for various applications [18]. The thermodynamic properties of the $ZrFe_2$—H_2 system have been thoroughly studied for the first time by Zotov et al. [19]. The absorption capacity they reported reached 1.7 wt.% and early all absorbed hydrogen can be desorbed reversibly, which makes this material a potential candidate for practical applications such as compression of hydrogen via metal hydride hydrogen compressors [21]. It has been also found that no change in cell symmetry occurs after the hydrogenation measurements, but on the other hand their equilibrium pressures are very high (ex. the absorption equilibrium pressure at room temperature is around 700 bar) [19]. To compensate for this, a commonly used method of changing the thermodynamic parameters of hydrides is the addition of substituting metals. This can be succeeded by either substituting the A or the B side of the chemical formula, in the AB_2 system, by other elements. In the current study, an investigation of the effect of partial substitution of Fe by V and Cr in $ZrFe_2$ alloys has been performed. These two intermetallic alloys have already been studied by other researchers [19,20], but only in comparison with a series of samples in the $ZrFe_{1.8}TM_{0.2}$ system (TM = transition metals). Zotov et al. [19] have studied a very large series of samples in the $ZrFe_2$ and $TiCr_2$ system, by partially substituting Fe or Cr by other elements, respectively. The results show that their hydrogenation and thermodynamic properties are directly affected by changes in the crystal structure, as a result of different quantities and elements substituted. Banerjee et al. [20] mainly focuses on the $ZrFe_{2-x}V_x$ system, trying to reveal the effect of Fe partial substitution of V, always remaining in the stoichiometric formula. In this case, SEM/EDX, XRD and hydrogen reaction measurement results have been investigated and once more again the hydrogen reaction properties

are in direct relation with the amount of Fe substituted by V. In our research work we have tried to focus on two samples and do a more exhaustive study in terms of microstructure observation by means of SEM and Rietveld analysis of the XRD patterns. These alloys have been synthesized by high frequency induction-levitation melting under Ar atmosphere. The characterization of the as-synthesized alloys has been observed by X-ray diffraction patterns (Rietveld Method) and Scanning Electron Microscopy (SEM). The hydrogen storage properties were measured by a Sievert-type apparatus at three different temperatures. The results showed almost the same uptake for the alloys after identical activation and lowering of the plateau pressure.

Experimental procedure

The alloys with the nominal composition $ZrFe_{1.8}V_{0.2}$ and $ZrFe_{1.8}Cr_{0.2}$ have been synthesized by 99.9% pure metals, by high frequency induction-levitation melting under pure Ar atmosphere (5N5). Before the melting procedure, the furnace chamber had been under vacuum with a turbo-molecular pump, until a value of $5 \cdot 10^{-5}$ mbar had been reached. To ensure homogeneity, the ingots were re-melted four times. The induction furnace was equipped with a water-cooled copper crucible that permits the rapid solidification of the alloy after the melting. As a result of the crystallization and the internal stresses that have been introduced during the rapid cooling process, an auto-occurred breaking of the ingots has been observed.

The crystal structures of the investigated alloys have been observed by X-ray diffraction (XRD) patterns and analyzed by the Rietveld analysis using Rietica Software [22]. Diffraction data of freshly crashed samples have been collected at room temperature on a PANalytical (Philips) − X'Pert MRD system, in the Bragg—Brentano geometry at $\lambda(Cu_{K\alpha}) = 0.15418$ nm, using the following conditions of $10 < 2\theta_B < 90°$ and a counting time and step of 10 s and 0.03°, respectively.

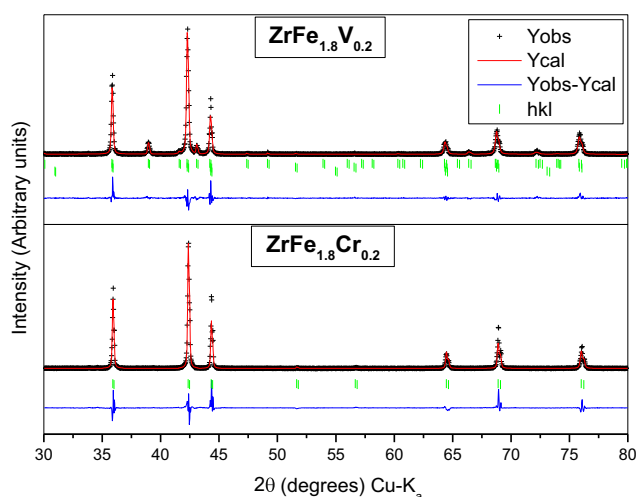The microstructure has been observed by a JEOL 840 A and 20 kV scanning electron microscope (SEM) on polished

Fig. 1 − Rietveld analysis of the XRD pattern of the $ZrFe_{1.8}V_{0.2}$ and $ZrFe_{1.8}Cr_{0.2}$ alloy.

Table 1 – Rietveld analysis results of the $ZrFe_{1.8}V_{0.2}$ and $ZrFe_{1.8}Cr_{0.2}$ alloy.

Samples	Space group (no.)	Phase	Lattice parameters (Å)		Cell volume (Å^3)	Phase abundance (wt.%)	Refinement parameter		
			a	c			R_p	R_{wp}	χ^2
$ZrFe_{1.8}V_{0.2}$	P63/mmc	C14	5.0199	8.2031	179.0257	0.30	15.84	22.48	2.073
	Fd-3m	C15	7.0954	–	357.2162	99.70			
$ZrFe_{1.8}Cr_{0.2}$	Fd-3m	C15	7.0816	–	355.1319	–	19.20	25.30	4.497
$ZrFe_2$ [15]	Fd-3m	C15	7.072	–	353.7	–	–	–	–

samples of the alloys, coupled with energy dispersive X-Ray analysis (Oxford ISIS 300 EDS).

The hydrogen storage properties of the alloys have been studied with a high pressure volumetric apparatus (SETARAM PCTPro-2000), at pressures up to 200 bar. The samples have been crushed into powder before insertion into the sample holder in ambient conditions. All pressure–composition–temperature (PCT) measurements have been obtained at 20, 60 and 90 °C. Two high temperature activation cycles have been conducted prior to PCT measurements. All preparation, activation and measuring conditions have been identical for both alloys, in order to eliminate the variables during their comparison.

Results and discussion

X-ray analysis

X-ray diffraction Rietveld analysis has been performed by using the RIETICA software [22] by starting from the space group and crystallographic data of a known formula that is near the examined one. Refinement of the crystallographic parameters of the materials by using the Rietveld analysis can be observed in Fig. 1. They exhibit similar diffraction patterns; the peaks of each reveal the dominant cubic C15 Laves phase structure, which may turn out to be the most favorable state in the case of Zr-based AB$_2$ compounds [23]. More specifically, a very small percentage of the hexagonal C14 Laves phase is present in the alloy with V, along with the main cubic C15 Laves phase, as it has been reported for similar compounds in the same family [22,24,25]. Due to the non-equilibrium solidification process of the induction melted ingots and the peritectic reaction during solidification in the pseudobinary system of V/Zr, it is not strange to observe minority phases

and solidification segregation in the as cast alloy [26]. Table 1 shows the values of the lattice parameters and the volume of unit cell for the two alloys. The atomic radius of the Cr(1.28 Å) is smaller than that of V(1.34 Å), thus substitution of Fe by Cr reduces the lattice parameters and the unit cell volume more than in the case of substitution of Fe by V.

SEM analysis

Microstructure analyses have been carried out by means of SEM, coupled with energy dispersive X-Ray analysis (EDX), and the results are shown in Fig. 2 and Table 2. As it is observed, two main regions are present in the $ZrFe_{1.8}V_{0.2}$ compound: the gray one, that is obviously the matrix, and the lighter regions which are poor to vanadium, comparing to other one. The main structure shows no significant deviations from the nominal formula, while the poor to vanadium regions probably explain the presence of the secondary hexagonal phase, as revealed by the X-Ray analysis. Similarly, the micrographs of the $ZrFe_{1.8}Cr_{0.2}$ compound show two differently lighted regions as well. However, the results of the EDX analysis indicate that the matrix (gray region) is not far away from the nominal stoichiometry while the lighter regions are almost pure zirconium.

Hydrogen storage properties

The hydrogen absorption/desorption isotherms of the two studied alloys are shown in Figs. 3 and 4. For both samples, two high temperature activation cycles have been conducted prior to PCT measurements. In a more specific manner, the alloys have been exposed to hydrogen pressure of 80 bar at 340 °C and then, an absorption process has taken place during the cooling of the absorbed sample down to 0 °C, with a cooling rate of 10 °C/min. Zotov et al. [19] reported that the
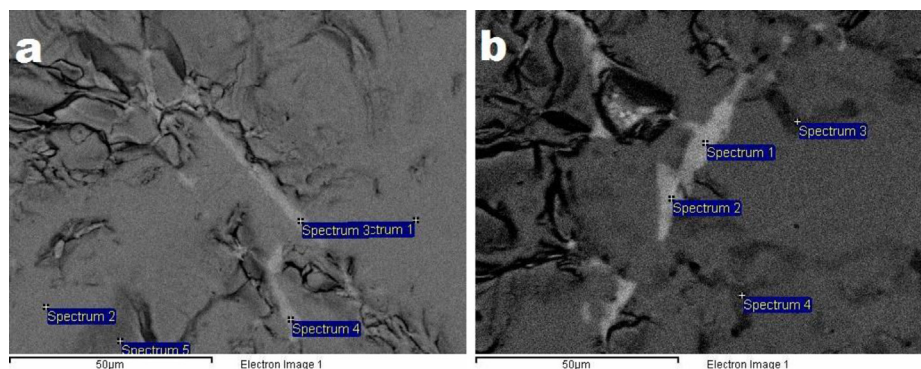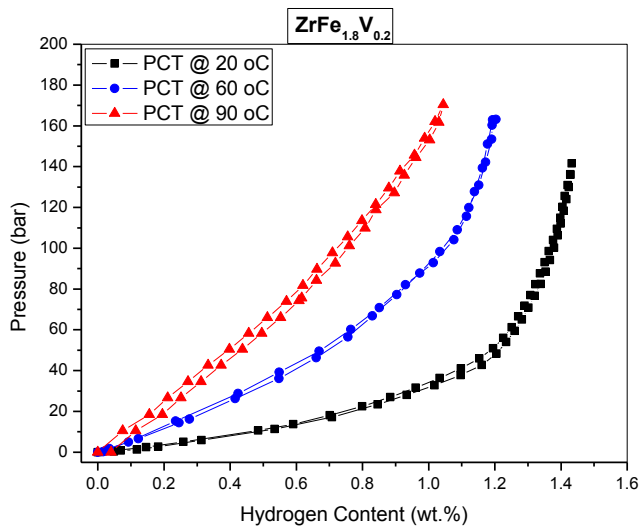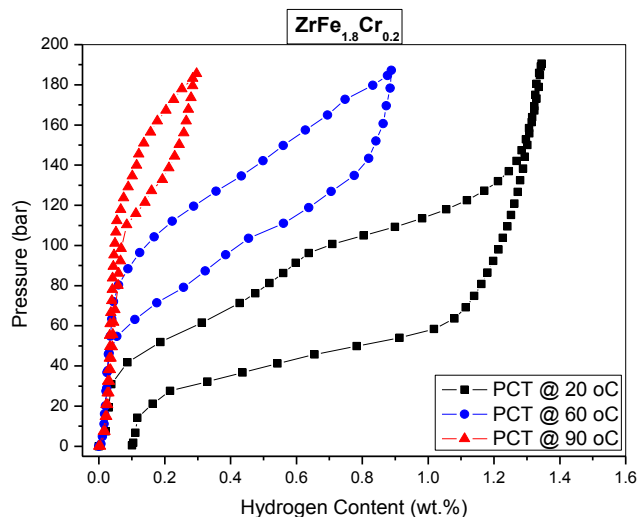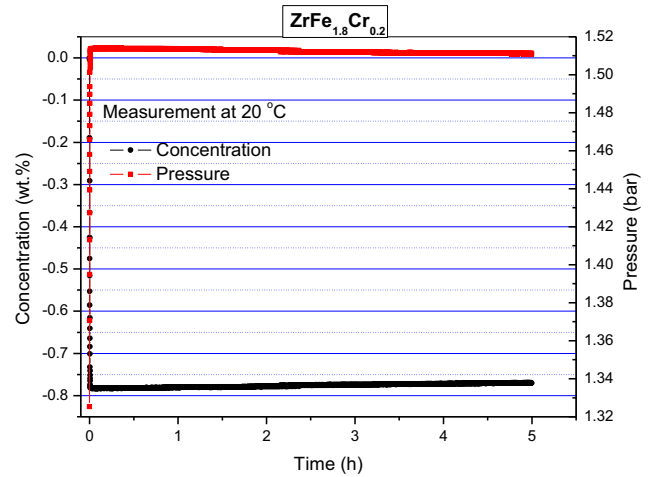

Fig. 2 – SEM micrographs of a) $ZrFe_{1.8}V_{0.2}$ and b) $ZrFe_{1.8}Cr_{0.2}$ alloy.

Table 2 – EDX analysis results of the as cast polished samples.

$ZrFe_{1.8}V_{0.2}$	V (wt.%)	Fe (wt.%)	Zr (wt.%)	Total
Spectrum 1	4.30	50.97	44.73	100
Spectrum 2	4.38	50.95	44.67	100
Spectrum 3	1.36	24.36	74.27	100
Spectrum 4	1.12	24.09	74.80	100
Spectrum 5	5.90	48.58	45.51	100
$ZrFe_{1.8}Cr_{0.2}$	Cr (wt.%)	Fe (wt.%)	Zr (wt.%)	Total
Spectrum 1	0.25	0.63	99.12	100
Spectrum 2	0	0.74	99.26	100
Spectrum 3	5.33	49.86	44.81	100
Spectrum 4	5.14	78.97	45.89	100

Fig. 5 – Desorption kinetics of a PCT measurement of the $ZrFe_{1.8}Cr_{0.2}$ compound.

Fig. 3 – P–C isotherms of $ZrFe_{1.8}V_{0.2}$ compound.

activation. Although, in the current work, the partial substitution of the V and Cr had a result in decreasing the equilibrium pressure for both absorption and desorption. During the activation procedure, a real time monitoring of the pressure has been observed in order a first sight of the hydrogen reaction within the alloys to be feasible. After ensuring the success of the activation process for both alloys, the samples have been under vacuum ($\sim 2 \cdot 10^{-3}$ mbar) at 90 °C for about 30 min prior to P–C–T measurements, that have been performed for both alloys at three different temperatures 20, 60 and 90 °C.

From Figs. 3 and 4, it can be extracted that the isotherms of the $ZrFe_{1.8}V_{0.2}$ compound are characterized by almost zero hysteresis and a pressure plateau that tends to be steeper as the measurement temperature rises. Moreover, its hydrogen uptake is reversible at all temperatures. It is observed that both alloys mainly crystallize in the cubic C15 Laves phase, with the V substitution sample having a larger unit cell volume and this explains the lower pressure plateau. They have shown almost

intermetallic $ZrFe_2$ compound starts to react with hydrogen at room temperature and pressure near 800 bar, while the absorption and desorption equilibrium pressure is 690 and 325 bar, respectively, at room temperature and after the

Fig. 4 – P–C isotherms of $ZrFe_{1.8}Cr_{0.2}$ compound.

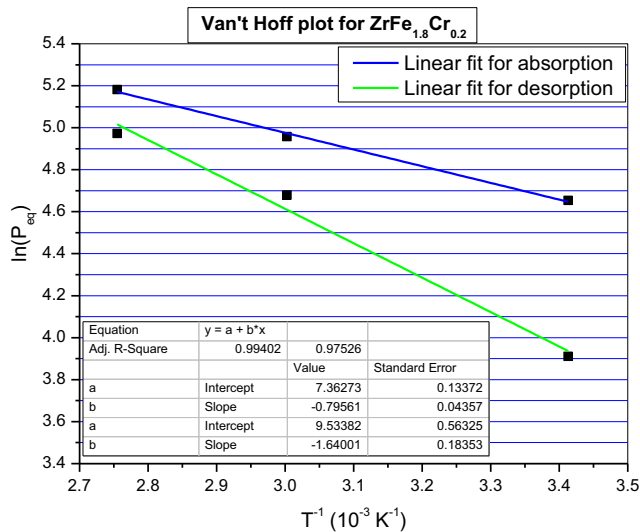| Equation	y = a + b*x		
Adj. R-Square	0.98968		
		Value	Standard Error
a	Intercept	9.70997	0.4285
b	Slope	-1.93836	0.13963

Fig. 6 – Van't Hoff plot for $ZrFe_{1.8}V_{0.2}$ compound.

Fig. 7 — Van't Hoff plot for $ZrFe_{1.8}Cr_{0.2}$ compound.

the same hydrogen uptake in pressures and are considered to be saturated. This could be explained by the fact that, for the intermetallic compounds with space group Fd3m, there are three types of tetrahedral coordinated interstitial sites available for hydrogen occupation, the 96g, 32e and 8b site (in Wyckoff notation). Since the g sites have the lowest energy, they are the first to be occupied upon hydrogenation, while the energy increases for the e sites, and finally for the b sites that have the highest. Since both investigated samples in our study have the same crystal structures and are saturated for the same temperature (in our case 20 °C) in the same narrow range of pressure, we may assume that hydrogen occupies the same sites, showing as a result the same hydrogen uptake.

On the other hand, isotherms of the compound where Fe is substituted by Cr exhibit a very intense hysteresis effect. Although its hydrogen capacity, once saturated, is not far away from that of $ZrFe_{1.8}V_{0.2}$ compound, all pressure plateaus have been shifted higher to about 60—70 bar. In addition, hydrogen that is absorbed at 20 °C is not fully reversible, leaving an amount of 0.1 wt.%, if the sample doesn't go under high dynamic vacuum for long time as the final desorption step. This could be explained by a non-complete activation procedure. Hydrogen pressure at 80 bar appears to be relatively sufficient for full hydrogen absorption near 0 °C. As a result, a part of the activation has been completed during the first isotherm at 20 °C, which probably explains this small amount of the irreversible hydrogen uptake and the change of the slope on the absorption curve at around 80—100 bar.

The most important criterion while measuring a PCT curve is the thermodynamic equilibrium, and the time allowed for

equilibrium is crucial in this respect. If not enough time is given to reach chemical equilibrium at each pressure point, the outcome is a reduced total capacity and a sloping equilibrium plateau [27—30]. Based on the previously mentioned time-to-equilibrium criterion, all our measurements have a real time monitoring of the pressure kinetics (and hence concentration since a volumetric method is used). In that way, the user can verify if equilibrium has been obtained for each individual point of the PCT curve and define the time allowed. For example, a part of the kinetics prior to time-to-equilibrium definition by the user is shown in Fig. 5. $ZrFe_2$-type Laves phase alloys are characterized by fast kinetics and therefore, pressure/concentration equilibrium of each point is reached after some minutes, as it was expected. Consequently, the slight change of the slope at the 20 °C curve of the $ZrFe_{1.8}Cr_{0.2}$ compound is explained by a non-complete activation procedure and not by non-sufficient time-to-equilibrium allowance.

The thermodynamics of the Zr—Fe—M ternary alloys have been calculated on terms of two important thermodynamic parameters namely, the molar enthalpy (ΔH) and molar entropy (ΔS) of the metal hydride. Since the hydrogen absorption—desorption plateau pressure of a metal hydride varies with temperature according to the well-known Van't Hoff equation,

$$lnP = \Delta H/RT - \Delta S/R \qquad (1)$$

the Van't Hoff plots have been used, which have been derived from the PCT data and shown in Figs. 6 and 7, to calculate those two physical magnitudes. Our results are in accordance to the references discussed in the manuscript and the modeling of relevant materials' properties [10]. The value of enthalpy is an index of stability of metal hydride. The higher value of ΔH shows a high degree of stability of hydride, low dissociation pressure and the requirement of rather high temperatures to decompose it to liberate hydrogen (Table 3).

Since vanadium and chromium have the same electronegativity (1.6 in the Pauling's scale) the moderation of the equilibrium pressures can't be directly explained by this. The atomic radii of Fe, Cr and V respect the following order, $R_V > R_{Fe} > R_{Cr}$, and one could assume that the same order would be followed from the unit cell volumes (all compounds have the C15 cubic structure — see Table 1). In contrast to that, V. Paul-Boncour et al. [26] and Zotov et al. [19] report a unit cell volume of $ZrFe_2$ which is the smallest, comparing to the other two compounds presented in this study. This means that by substituting Fe by V or Cr, we achieve to increase the unit cell volume of the dominant cubic C15 Laves phase in both cases, which has a direct effect in decreasing the equilibrium pressure of the reference $ZrFe_2$ compound. Moreover, this

Table 3 — Hydrogen sorption properties of the $ZrFe_{1.8}V_{0.2}$ and $ZrFe_{1.8}Cr_{0.2}$ alloy.					
Alloy	$P_{a/d\ 20\ °C}$[a] (bar)	$P_{a/d\ 90\ °C}$[a] (bar)	$ln(P_a/P_d)_{20\ °C}$	$\Delta H_{a/d}$ (kJ/mol H_2)	$\Delta S_{a/d}$ (J/K mol H_2)
$ZrFe_{1.8}V_{0.2}$	22.5/22.5	81.7/81.7	—	−16.11/16.11	80.72/80.72
$ZrFe_{1.8}Cr_{0.2}$	104.9/49.9	177.9/144.4	0.74	−6.61/13.63	61.19/79.23
[a] Pressures for absorption and desorption are referring to equilibrium pressures of each isotherm.					

decrease of the equilibrium pressure of the parent $ZrFe_2$ compound, as a result of the unit cell volume, has a strong dependence on the order of the unit cell volumes, as presented in Table 1, as well as on the filling of the 3d bands ($3d^6$, $3d^5$ and $3d^3$ for Fe, Cr and V, respectively).

Conclusions

Two intermetallic compounds with $ZrFe_{1.8}M_{0.2}$ (M = V, Cr) formula were successfully synthesized by the induction-levitation melting process. Rietveld analysis of the XRD patterns for both compounds reveals that they have been crystallized in the cubic C15 Laves phase. Hydrogen storage properties V substituted AB_2 sample show that the hydrogen sorption plateau pressure decreases compared to the Cr substituted sample. Moreover, the compound with Cr shows a very large hysteresis effect while in the meantime the V substituted sample has zero hysteresis. Both compounds show similar maximum hydrogen uptake after identical activation procedure before all absorption/desorption measurements. The hydrogen storage properties reveal that both $ZrFe_{1.8}V_{0.2}$ and $ZrFe_{1.8}Cr_{0.2}$ intermetallic compounds have a lower plateau pressure compared to the parent $ZrFe_2$ alloy and show reasonable storage capacity.

Acknowledgments

REFERENCES

[1] Princini G, Agresti F, Maddalena A, Lo Russo S. The problem of solid state hydrogen storage. Energy 2009;34:2087–91.

[2] Ross DK. Hydrogen storage: the major technological barrier to the development of hydrogen fuel cell cars. Vacuum 2006;80:1084–9.

[3] Makridis SS, Gkanas EI, Panagakos G, Kikkinides ES, Stubos AK, Wagener P, et al. Polymer-stable magnesium nanocomposites prepared by laser ablation for efficient hydrogen storage. Int J Hydrogen Energy 2013;38:11530–5.

[4] Züttel A. Materials for hydrogen storage. Mater Today 2003;6:24–33.

[5] Semenenko KN, Sirotina RA, Savchenkova AP, Burnasheva VV, Lototskii MV, Fokina EE, et al. Interactions of _3-ScFe2 and _2-ScFe1.8 with hydrogen. J Less Common Met 1985;106:349–59.

[6] Akiba E, Iba H. Hydrogen absorption by Laves phase related BCC solid solution. Intermetallics 1998;6(6):461–70.

[7] Fukai Y. The metal hydrogen system. Berlin: Springer; 1993.

[8] Filipek SM, Jacob I, Paul-Boncour V, Percheron-Guegan A, Marchuk I, Mogilyanski D, et al. Investigation of $ZrFe_2$ and $ZrCo_2$ under very high pressure of gaseous hydrogen and deuterium. Pol J Chem 2001;75:1921–6.

[9] Bulyk II, Basaraba YB, Dovhyj YO. Influence of Ti on the hydrogen induced phase-structure transformations in the $ZrCr_2$ intermetallic compound. Intermetallics 2006;14(7):73541.

[10] Gkanas EI, Makridis SS, Stubos AK. Modeling and simulation for absorption–desorption cyclic process on a three-stage metal hydride hydrogen compressor. Comput Aided Proc Eng 2013;32:379–84.

[11] Koultoukis ED, Gkanas EI, Makridis SS, Christodoulou CN, Fruchart D, Stubos AK. High-temperature activated AB_2 nanopowders for metal hydride hydrogen compression. Int J Energy Res 2014;38:477–86.

[12] Jain A, Jain RK, Agarwal S, Ganesan V, Lalla NP, Phase DM, et al. Synthesis, characterization and hydrogenation of $ZrFe_{2−x}Ni_x$ (x=0.2, 0.4, 0.6, 0.8) alloys. Int J Hydrogen Energy 2007;32:3965–71.

[13] Sakintura B, Lamari-Darkrim F, Hirscher M. Metal hydride materials for solid hydrogen storage: a review. Int J Hydrogen Energy 2007;32:1121–40.

[14] Kuriiwa T, Tamura T, Amemiya T, Fuda T, Kamegawa A, Takamura H, et al. New V-based alloys with high protium absorption and desorption capacity. J Alloys Compds 1999;293–295:433–6.

[15] Sinha VK, Wallace WE. The hyperstoichiometric $ZrMn_{1+x}Fe_{1+y}$–H_2 system I: hydrogen storage characteristics. J Less-common Met 1983;91:229–37.

[16] Kandavel M, Ramaprabhu S. Hydriding properties of Ti substituted non-stoichiometric AB2 alloys. J Alloys Compd 2004;381:140–50.

[17] Kojima Y, Kawai Y, Towata SI, Matsunaga T, Shinozawa T, Kimbara M. Development of metal hydride with high dissociation pressure. J Alloys Compd 2006;419:256–61.

[18] Naik Y, Ramarao GA, Venugopal V. Zirconium–cobalt intermetallic compound for storage and recovery of hydrogen isotopes. Intermetallics 2001;9:309–12.

[19] Zotov TA, Movlaev EA, Mitrokhin SV, Verbetsky VN. Interaction in (Ti, Sc)Fe_2–H_2 and (Zr, Sc)Fe_2–H_2 systems. J Alloys Compd 2008;459:220–4.

[20] Banerjee S. Studies on advanced materials for hydrogen storage; 2013 [Ph.D. thesis of Homi Bhabha National Institute].

[21] http://www.rietica.org/.

[22] Zotov TA, Sivov RB, Movlaev EA, Mitrokhin SV, Verbetsky VN. IMC hydrides with high hydrogen dissociation pressure. J Alloys Compd 2011;509:S839–43.

[23] Van Midden HJP, Prodan A, Zupanic E, Zitko R, Makridis SS, Stubos AK. Structural and electronic properties of the hydrogenated $ZrCr_2$ Laves phases. J Phys Chem 2010;114:4221–7.

[24] Koultoukis ED, Makridis SS, Fruchart D, Stubos AK. Two-stage hydrogen compression using Zr-based metal hydrides. Solid State Phenom 2013;194:249–53.

[25] Zhang TB, Wang XF, Hu R, Li JS, Yang XW, Xue XY, et al. Hydrogen absorption properties of $Zr(V_{1−x}Fe_x)_2$ intermetallic compounds. Int J Hydrogen Energy 2012;37:2328–35.

[26] Paul-Boncour V, Bourée-Vigneron F, Filipek SM, Marchuk I, Jacob I, Percheron-Guégan A. Neutron diffraction study of ZrM_2D_xdeuterides (M=Fe, Co). J Alloys Compd 2003;356–357:69–72.

[27] Rouquerol J, Avnir D, Fairbridge CW, Everett DH, Haynes JH, Pernicone N, et al. Recommendations for the characterization of porous solids. Pure Appl Chem 1999;99:1739–58.

[28] Broom D. The accuracy of hydrogen sorption measurements on potential storage materials. Int J Hydrogen Energy 2007;32:4871–88.

[29] Zlotea C, Moretto P, Steriotis T. A round Robin characterisation of the hydrogen sorption properties of a carbon based material. Int J Hydrogen Energy 2009;34:3044–57.

[30] Moretto P, Zlotea C, Dolci F, Amieiro A, Bobet J-L, Borgschulte A, et al. A round Robin test exercise on hydrogen absorption/desorption properties of a magnesium hydride based material. Int J Hydrogen Energy 2013;38:6704–17.